Electron heating effects in free-standing single-crystal GaAs fine wires

1990 J. Phys.: Condens. Matter 2 1817

(http://iopscience.iop.org/0953-8984/2/7/012)

J. Phys.: Condens. Matter **2** (1990) 1817–1825. Printed in the UK

Electron heating effects in free-standing single-crystal GaAs fine wires

A Potts, M J Kelly†, C G Smith, D G Hasko, J R A Cleaver, H Ahmed, D C Peacock†, D A Ritchie, J E F Frost and G A C Jones

Cavendish Laboratory, Department of Physics, University of Cambridge, Madingley Road, Cambridge CB3 0HE, UK

Received 24 July 1989, in final form 25 October 1989

Abstract. We report on experiments, and their analysis, on electron heating effects in 3.2 μm long free-standing fine wires (triangular cross-section with $\simeq$0.5 μm side) of single-crystal GaAs doped at 10^{17} cm^{-3}. The data can be used to extract a thermal conductivity that has a linear temperature dependence, consistent with a contribution from electrons and/or one-dimensional phonons. We show that the electronic contribution dominates.

1. Introduction

The physics of free-standing fine wires has all the ingredients of one-dimensional electronic behaviour as realised in other systems, e.g. fabricated conduction channels in semiconductor multilayer structures (Wharam *et al* 1988, Smith *et al* 1988, Reed *et al* 1988), and fine metallic interconnects (Beutler and Giordano 1988), etc., with the added feature that the lattice vibrational modes are confined at least in their lateral propagation. In our previous studies of free-standing wires, the amorphous nature of silicon nitride (Lee *et al* 1984) would have resulted, and the polycrystalline nature of gold–palladium alloys (Smith and Wybourne 1986) actually did result, in very short mean free paths for the phonons. These in turn masked any of the specifically one-dimensional phonon effects on the thermal properties of such wires, as predicted by Kelly (1982). (See also Jackle (1981) and Maynard and Akkermans (1985).) Even in alloy wires with 30 nm diameter, the results of electron heating experiments (measurements of the electrical resistance as a function of current) could be explained satisfactorily by invoking the Weidemann–Franz law to relate the electrical and thermal conductivity, and allowing the heat generated in the wires to be conducted out through both ends. The measured changes in the resistance were quite modest, so changes in the thermal conduction processes would be hard to extract, in contrast to the situation described below.

In order to see any quasi-one-dimensional phonon transport, as opposed to the more readily observed electronic effects, it has been appreciated that single-crystal wires are essential. When one considers the fabrication processes of epitaxial deposition, fine-line lithography, and plasma or other etching techniques, the range of materials suitable for the production of single-crystal fine wires is limited. We have recently succeeded in

† Also at GEC Hirst Research Centre, East Lane, Wembley HA9 7PP, UK.

0953-8984/90/071817 + 09 $03.50

fabricating free-standing wires of GaAs (Hasko *et al* 1988) etched from material doped at 10^{17} cm^{-3} deposited on semi-insulating GaAs, and have undertaken basic low-temperature transport and magnetotransport studies. These confirm that in triangular wires of order 0.5 μm side, the depletion in from the side-walls leaves a conducting channel of order 0.12 μm diameter. The temperature dependence of the resistance is consistent with one-dimensional weak localisation and three-dimensional electron–electron interactions dominating the quantum corrections to the Boltzmann conductivity (for details of the transport experiments and their interpretation, see the companion paper, Potts *et al* 1990).

Our present structure is already in an interesting regime as far as thermal transport is concerned. Measurements of the thermal conductivity of GaAs at low temperatures, and over a range of doping that spans our value (Holland 1963, 1964), indicate that boundary scattering of phonons limits the low-temperature thermal conductivity in samples with lateral dimensions of order 0.5 cm, and that the doping has its main effect in limiting the maximum conductivity at near liquid nitrogen temperatures. Our samples have lateral dimensions 10^4 times smaller. The precise measurements of thermal properties have always been a much more difficult task than their electrical counterparts, and so in this paper we discuss a series of experiments on electron heating. The resistance of free-standing wires was measured and analysed at five different lattice temperatures (between 0.47 K and 4.2 K) as the current was increased. Here we can easily achieve a 25% change in the resistance as the current is increased to typically 50 nA through each of 27 wires in parallel.

The plan of the present paper is as follows: in the next section we give a brief summary both of the structures used in these experiments and the method of their fabrication. We also review the results of previous transport measurements in so far as they are invoked for the present study. In the subsequent sections we describe (i) the electron heating experiments, (ii) a solution to the relevant thermal transport equations, (iii) an analysis of the experimental results, and (iv) the implications of this analysis. We find that a model invoking electron heating is able to account for the data within the accuracy of the measurements.

2. Fabrication of free-standing wires

The gallium arsenide free-standing wire sample consisted of thirty identical parallel wires, each of 3.2 μm length and 0.5 μm width, connecting a pair of pads, and each pad had two ohmic contacts to permit quasi-four-terminal electrical measurements. These were fabricated using a combination of electron beam lithography and wet chemical etching (Hasko *et al* 1988). PMMA resist on a (001)GaAs surface was patterned to give stripes of resist parallel to the [001] direction; this was then used as an etch mask for use with a 10 : 1 citric acid/hydrogen peroxide etch. This anisotropic etch gives an undercut profile revealing slow-etching {221}A and {111}A planes. As the etching proceeds, the resist bar is undercut and leaves a free-standing triangular section of GaAs. The slow-etching planes yield very smooth and uniform surfaces to the wire, this being important in the reduction of scattering processes in subsequent transport experiments. Wires have been fabricated using a 1 μm thick epitaxial layer of GaAs doped at 10^{17} cm^{-3} Si, which was grown by MBE on a semi-insulating wafer. Isolation was achieved by choosing an etched depth that was greater than the epitaxial layer thicknesses and by etching a trench around the contact pads and wires. Ohmic contacts were made using AuGePd and were

rapidly sintered; these also acted as bond pads. The conducting area of the wire is less than the total cross-sectional area due to surface depletion, and this results in an approximately circular conducting section of diameter $\simeq 125$ nm for wires of this size and doping. Inspection of the structure in an SEM indicated that 3 of the 30 wires had broken, or were too thin to conduct, and we assume that 27 wires are conducting.

3. Previous transport studies

Detailed low-temperature and magnetoresistance measurements have been made on this sample and the results (Potts *et al* 1990) are used as inputs to the analysis of the electron heating experiments performed here. An AC lock-in technique was used to measure the resistance of the sample with sensing currents of 0.3 nA per wire, so as to avoid any of the self-heating effects that we examine in this paper. Between 0.475 K and 4.2 K, the conductance per unit length of the sample increases logarithmically with temperature:

$$G(T) = 2.79(1 + 0.1016 \ln(T/\mathrm{K})) \times 10^{-9}\ \Omega^{-1}\mathrm{m}. \tag{3.1}$$

This leads to approximately a 20% variation of resistance over the temperature range, which is used as a 'thermometer' in the experiments below. Further measurements were made up to 10 K, with broadly a similar temperature dependence being followed, a fact that is important in sections 6 and 7 below. While a logarithmic variation with temperature is usually characteristic of two-dimensional electron transport, a further analysis of the details of the dependence of the resistance on both magnetic field and temperature leads to a clear identification of one-dimensional weak localisation as being responsible for 70% of the temperature dependence, and the remainder coming from three-dimensional electron–electron interactions. In the analysis in section 7, we account for the three-dimensional character of the electron motion. The analysis leads to a consistent interpretation of the data using parameters for the diffusion constent of the electrons, the relevant screening parameters, the characteristic scattering lengths for the electrons, and the recent theories of quantum interference in reduced-dimensionality semiconductors. Having established the physical origin of the temperature variation of the conductance, we can appeal to this during the interpretation of the data we present in the following sections.

4. The electron heating experiments

Whereas the sensing current was kept low in the measurements of the resistance as a function of lattice temperature in the previous section, the experiments were repeated with currents of up to 50 nA in each wire. The resistance of the sample as a function of current, $R(I)$, fell by as much as 20% with rising current, consistent with a rising temperature in the centre of the wire. Experiments were carried out between 0.475 K and 4.2 K, with qualitatively the same behaviour being seen throughout. The measurements were carried out as follows: a DC bias in series with a 10 mV AC signal is passed through a 1 MΩ resistor, which in turn is in series with the sample. Four-terminal measurements of the AC differential resistance were made using standard phase sensitive detection techniques. The AC sensing current is again of order 0.3 nA per wire.

5. Heat conduction in fine wires

We set out to solve the following heat conduction equation for the temperature distribution $T(x)$ along a free-standing wire between $x = 0$ and $x = L$:

$$-(\mathrm{d}/\mathrm{d}x)((K(T)A\,\mathrm{d}T/\mathrm{d}x) = \text{power generated per unit length} = I^2\rho(x)/A \tag{5.1}$$

where A is the cross-section of the wire, I the current in the wire, $\rho(x) = \rho(T(x))$ the resistivity along the wire, assumed to have a value determined by the local temperature, and $K(T)$ the three-dimensional thermal conductivity: if we multiply $K(T)$ and A together, the result is the equivalent 1D thermal conductivity which features in the sections below. Already one problem is raised: strictly, if we consider the electronic contribution to the thermal transport, the cross-sectional area is that of the conducting channel, while if we consider the lattice contribution, the area on the left-hand side of (5.1) is that of the whole wire. Ultimately there is a factor of 2–4 in the samples considered here, but we can avoid the problem since the combination $\rho(x)/A$ on the right-hand side of equation (5.1) is equal to $R(x)/L$, and resistances and lengths are available experimentally in the case of low currents where electron heating is assumed negligible. From the earlier transport studies (Potts *et al* 1990), we write the resistivity using the form for the conductance given in section 3. Using T_0 as the lattice temperature in the contacts, and T the excess local temperature, we consider two forms of the thermal conductivity writing (i) $K = \eta(T_0 + T)$ for the electronic case where η is assumed to contain the specific heat factor (which also provides the linear temperature dependence), the mean velocity and mean free path terms, all for the electrons, and (ii) $K = \lambda(T_0 + T)^3$ for the lattice contribution if we assumed the bulk **3D** lattice conductivity were to apply (see Ashcroft and Mermin (1976) for details of both forms of the thermal conductivity), and that the electron–phonon interactions is sufficient for both electrons and phonons to be in equilibrium with each other along the wires. It should also be noted that if 1D lattice conduction dominates the heat transfer, the analytic structure of solution (i) applies, as the temperature dependence comes entirely from the specific heat term which is linear in temperature in 1D, but where the η is now of phonon origin, containing elastic constants, densities etc. (see Kelly 1982 for details). The method of solution of the differential equation is the same in the two cases. If we define in the respective cases (i) $y(x) = (T(x) + T_0)^2$ and (ii) $z(x) = (T(x) + T_0)^4$, then equation (5.1) becomes (i)

$$-\mathrm{d}^2y/\mathrm{d}x^2 = -\varphi_y I^2 1/[1 + (\beta/2)\ln(y(x))] \tag{5.2a}$$

or (ii)

$$-\mathrm{d}^2z/\mathrm{d}x^2 = -\varphi_z I^2 1/[1 + (\beta/4)\ln(z(x))] \tag{5.2b}$$

where $\varphi_y = 2R_0/\eta L$ and $\varphi_z = 4R_0/\lambda L$, where L is the wire length, and R_0 is the characteristic resistance of the problem, obtained from the 1 K value of $G(T)$ in the previous section. β is the coefficient of the ln T term in (3.1). We solve the equations for φ_y and φ_z numerically, subject to the boundary conditions that $T = T_0$ at both $x = 0$ and $x = L$. We assume that, with a profile for $T(x)$, we can define a local contribution to the resistance and hence obtain the resistance of the wires as

$$R_\varphi(I) = \int \rho(T_\varphi(x))\,\mathrm{d}x/A. \tag{5.3}$$

In fact, in the subsequent fitting of the experimental data, we minimise as a function of φ the expression

$$\Sigma(R(I)_{\mathrm{exp}}/R_{\mathrm{exp}}(I = 0) - R_\varphi(I)/R_\varphi(I = 0))^2 \tag{5.4}$$

the sum being taken over all the data points for different currents. If we examine

Table 1. Fit to a linear temperature dependence; $K = \eta T$.

Lattice temperature (K)	0.47	0.81	1.02	1.25	4.2
$\langle\varphi_y\rangle$ from fit	1.18	0.96	0.84	0.71	0.85
Residual (%)	0.15	0.08	0.04	0.04	0.05

Table 2. Fit to a cubic temperature dependence; $K = \lambda T^3$.

Lattice temperature (K)	0.47	0.81	1.02	1.25	4.2
$\langle\varphi_z\rangle$ from fit	1.12	1.82	2.21	2.59	32.2
Residual (%)	0.4	0.09	0.04	0.05	0.05

equations (5.1)–(5.4) we see that all the symbols are either fixed temperatures (T_0, known from the experimental conditions) or are independently measured (such as current, wire length or low-current resistance) except for φ, and it is with respect to the combination of constants in φ that we minimise the sum in equation (5.4). In fact φ is basically a measure of the relative electrical and thermal capacities of the wire, expressing the scale of temperature rise that a given current can produce. While we discuss the physics in the next section, we note here that the fitting procedure gives unique and stable solutions for φ. Viewed purely as a fitting problem, the residuals per data point are less than 1%. For reasons of numerical accuracy, the units of current and length in the calculations are 1 nA and 10 μm respectively, and the renormalised value of φ in these new units, written $\langle\varphi\rangle$, is of order unity. (Note: this scaling of current and length, by factors of 10^9 and 10^5 respectively, leads to a 10^{28} correction factor to be applied to obtain the value of φ in SI units, because of the $I^2\,\mathrm{d}x^2$ combination in equations (5.1) and (5.2).) The results below show a comparable fit, over the entire temperature range, to a ηT and a λT^3 form for the thermal conductivity.

6. Fitting analysis of the heating experiments

In tables 1 and 2 we summarise the results of the fitting of theory and experiment. In figure 1, we show the fits to the experiments for both the linear and cubic temperature dependence. One sees from the constancy of $\langle\varphi_y\rangle$ how much better a linear temperature dependence is for the thermal conductivity: indeed the temperature dependence of $\langle\varphi_z\rangle$ is consistent with trying to force a linear temperature dependence on K. The residual fitting errors are marginally better for a linear temperature fit. Taking the average value of $\langle\varphi_y\rangle \simeq 0.9$ from the above data, $R_0 = 31$ kΩ extracted from the data for 27 wires in parallel, and a length of 3.2 μm, we extract a value for $\eta = 2.1 \times 10^{-18}$ SI units (W m K^{-2}), with an $\simeq$20% error.

In figure 2, we plot the temperature profile for the higher levels of currents used in experiments with lattice temperature of 0.47 K. We see (i) a substantial temperature rise to 5.2 K (with a rise to 7.5 K when the lattice temperature is 4.2 K) showing that the wires are driven far from their ambient condition, and (ii) that the temperature variation of the thermal conductivity results in a rather flatter temperature distribution than the parabolic form $\sim x(L - x)$ expected if the thermal conductivity were constant: the temperature in the middle would rise to 8.83 K instead of 4.51 K if a constant thermal

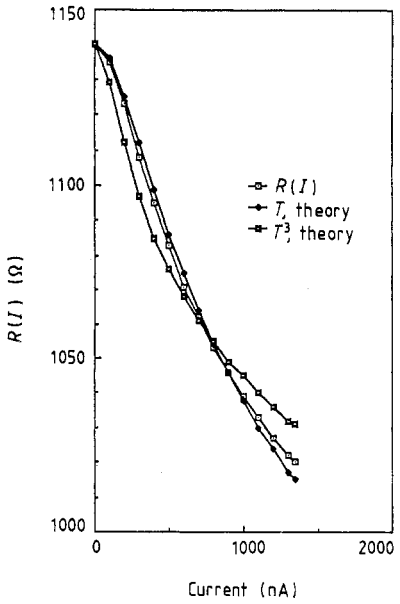

Figure 1. The experimental data and theoretical fits for an intermediate lattice temperature of 1.02 K.

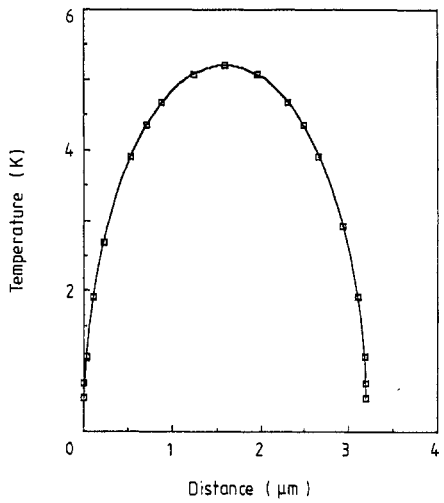

Figure 2. A plot of the temperature profile for maximum current for the case of a lattice temperature of 0.47 K, but with approximately 50 nA passing through each wire.

conductivity, evaluated at the lattice temperature were used. The fact that good agreement can be achieved with a one-parameter fit implies that the form of the temperature dependence $G(T)$ in equation (3.1) holds well over the 0.5–10 K range, and possibly that electron heating is a major contribution to the explanation of the results.

7. Implications

We consider now the possible thermal conduction mechanisms and how they could explain the fit to the data.

7.1. Linearly T-dependent thermal conductivity; electronic contribution

We can evaluate the Wiedemann–Franz ratio for our system, to see to what extent the electronic contribution to the thermal conductivity is sufficient to explain our results. We obtain a one-dimensional electrical conductivity from the experimental data as

$$\sigma_{1D} = L/R = 1.03 \times 10^{-10}\ \Omega^{-1}\ \mathrm{m}$$

where R is the resistance of one wire, and L its length. In our case we would deduce a Lorenz number

$$\mathcal{L} = K/\sigma T = \eta/\sigma = 2.1 \times 10^{-8}\ \mathrm{W}\,\Omega\,\mathrm{K}^{-2}$$

which is within 20% (cf. the confidence of our estimate for η) of the value of 2.44×10^{-8}

that would allow us to explain the results solely in terms of electronic contributions to the thermal conductivity. While we might invoke some phonon contribution to the thermal transport, it is clear that the electronic contribution is the most important ingredient. At first sight this is surprising as, in comparison with metals, there are very few carriers present, and one might expect a much smaller electronic contribution to the thermal conductivity.

7.2. Linearly T-dependent thermal conductivity; 1D lattice contribution

The dominant phonon wavelength of a black-body distribution at temperature T(K) is given by 100 nm/T, so that at the lowest temperatures, we have O(10) 1D phonon subbands excited, a number that rises to O(10^3) at the highest temperature. In a clear search for phonon effects in the present samples, we should reduce the temperature to $\simeq$ 200 mK. In a 1D Debye theory, the specific heat per 1D phonon branch is $(\pi k_B)^2 T/(3hc)$ where c is the speed of sound, and k_B the Boltzmann constant. The thermal conductivity can be written as $K = (\pi k_B)^2 \lambda_p T/(3h)$, where λ_p is the phonon mean free path. This gives $K \sim 6 \times 10^{-12} \lambda_p T$(W m K^{-1}) per branch. Given our value of η above, and assuming only phonons contribute, our results would imply a product, $N_B \lambda_p$, of the number of (lateral) phonon branches participating in the thermal conduction multiplied by the phonon mean free path of only 0.6 μm. Not only does this lead to a very short mean free path, but the temperature independence of η implies that there is an (unlikely) cancellation between the temperature dependences of the number of lateral branches participating and the mean free path of the phonons. The electronic mechanism provides a neater explanation.

7.3. Further analysis

We can take our analysis of the data several stages further. To do so, we estimate relevant transport length and time scales. A phonon emitted in the middle of our wire takes $\simeq$ 0.5 ns to escape if it travels at the speed of sound. The time for an electron to diffuse from the centre of the wire to either end is $\tau_{exit} \simeq 12$ ns. The magnetotransport data of Potts *et al* (1980) have been analysed to infer an inelastic scattering length for electrons of $\simeq$0.2 μm, and the conductivity implies an elastic scattering length of $\simeq$10 nm. We can use the data of Holland (1963, 1964) on macroscopic samples of GaAs with doping comparable to ours to infer a boundary limited phonon mean free path of $\simeq$0.5 cm. This implies an intrinsic electron–phonon scattering time τ_{ep} in excess of 1.2 μs in his experiments. If we assume that this characteristic time is not greatly different for our much smaller sample, then $\tau_{ep} > \tau_{exit}$. A hot electron in the middle of the wire will diffuse out in 1/100 of the time it would take to emit a phonon. Any phonon that was produced would escape the wire in less than 10^{-3} of the time before another phonon is emitted.

In this regime the lattice remains cold—only the electrons are heated. The electron–electron scattering will thermalise the electrons over a distance of 0.2 μm, so electrons near the end of the wire will be cooler than those in the middle. This is quite different from what one normally expects, because the heat is being lost from the middle of the wire by the electron thermal conductivity to the cold electrons at the ends. Normally the hot electrons in a large sample (large in comparison with the electron–phonon scattering length for electrons) lose their energy to the phonons. In our case we can ignore the phonon bath except in as much as it contributes to cooling electrons at either end. In

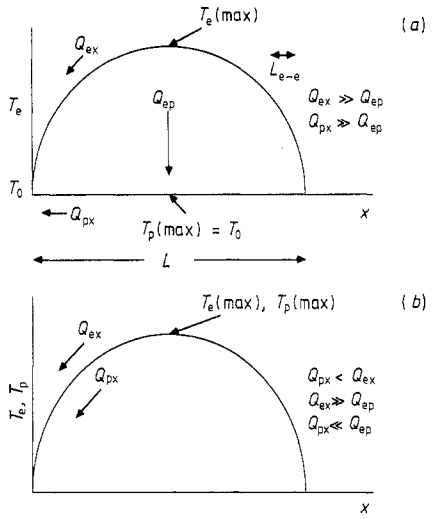

Figure 3. A schematic diagram of the temperature profile showing the heat transfers Q_{ex} (Q_{px}) from electrons (phonons) exiting from the wire, and Q_{ep} from electrons to phonons, in the regime of (*a*) delocalised, and (*b*) localised phonons. In both cases T_e(max) is determined by the thermal conductivity of the electrons. In (*a*) the lattice stays cold, and heat is conducted out by diffusion of hot electrons into the cold electron baths at either end, while in (*b*) the lattice does warm to the local electron temperature, but the localised phonons are ineffective in carrying away the excess energy. Our estimates would imply that the situation in (*a*) applies.

figure 3(*a*) we show the situation we have just described, while in figure 3(*b*) we show an alternative explanation if all the phonons were localised, but even in this case, the heat loss and therefore temperature profile is set up by the thermal conduction of the electrons.

7.4. Other work

Taylor *et al* (1989) have measured electron heating effects on submicrometre n^+-GaAs wires that still remain on a semi-insulating GaAs substrate. Although they use an electron heating model, their detailed analysis differs from ours in not being able to use the thermal conductivity because of the large thermal reservoir of the substrate. They obtain a temperature-independent energy relaxation time, and invoke by way of explanation a series of near-elastic scattering events at the surface of the wires. It would be tempting to analyse their data, which are qualitatively similar to ours, with a purely electronic heating mechanism, leaving the phonon and other relaxation processes to their contact regions. In earlier work on nearly free-standing (sub-micrometre diameter) wires of the same 10 μm length as those used by Taylor *et al*, we obtained similar data to those reported in this paper, so even on this scale, the phonons play at most a modest role in the thermal transport in comparison with the electrons. Our limited range of temperature and magnetic fields at present relate to measurements on free-standing samples, in which a vacuum environment is essential: the samples are not expected to withstand intimate contact with turbulent or viscous fluids as occurs in most other transport studies of quasi-one-dimensional systems.

8. Summary

In summary, although we have persisted in our search for quasi-1D phonon transport phenomena, it seems in the present case, even for wires of 0.5 μm diameter, the system is strongly influenced by electron heating effects that mask any specifically phonon effects in the 0.4–4 K regime over which the experiments are performed. If they could be performed on a gated sample in the millikelvin range, we would expect a sharp drop in the electrical conductivity as a metal–insulator regime is induced for the electrons, and a different form of temperature dependence of $G(T)$ would follow. With few lateral phonon branches being excited at these very low temperatures, and with strongly localised electrons, the results of electron heating might allow the one-dimensional phonon contribution to the thermal conductivity to be unmasked. Note finally the possibility of carrying out experiments on a free-standing heterojunction: if the very high electron mobilities in the two-dimensional electron gas survive the fabrication process, the ballistic motion of carriers in wires of (say) 5–10 μm, at least for low heating currents, should enable the energy to be swept out of the wire, resulting in very small temperature rises. If the short phonon mean free paths inferred in section 7.2 above were still to apply, quasi-one-dimensional phonon transport may remain elusive.

Acknowledgments

A Potts, D G Hasko and C G Smith are supported by SERC (UK). A Potts is a CASE student with GEC. MJK holds a Royal Society/SERC Industrial Fellowship.

References

Ashcroft N W and Mermin N D 1976 *Solid State Physics* (New York: Holt, Rinehart and Winston)
Beutler D E and Giordano N 1988 *Phys. Rev.* B **38** 8–19
Hasko D G, Potts A, Cleaver J R A, Smith C G and Ahmed H 1988 *J. Vac. Sci. Technol.* B **6** 1849–51
Holland M G 1963 *Phys. Rev.* **132** 2461–71
—— 1964 *Phys. Rev.* **134** A471–80
Jackle J 1981 *Solid State Commun.* **39** 1261–3
Kelly M J 1982 *J. Phys. C: Solid State Phys.* **15** L969–73
Lee K L, Ahmed H, Kelly M J and Wybourne M N 1984 *Electron. Lett.* **20** 289–91
Maynard R and Akkermans E 1985 *Phys. Rev.* B **32** 5440–2
Potts A, Hasko D G, Cleaver J R A, Smith C G, Ahmed H, Kelly M J, Frost J E F, Jones G A C, Peacock D C and Ritchie D A 1990 *J. Phys.: Condens. Matter* **2** 1807
Reed M A, Randall J N, Aggarwal R J, Matyi R J, Moore T M and Wetsel A E 1988 *Phys. Rev. Lett.* **60** 535–8
Smith C G, Pepper M, Ahmed H, Frost J E F, Hasko D G, Peacock D C, Ritchie D A and Jones G A C 1988 *J. Phys. C: Solid State Phys.* **21** L893–8
Smith C G and Wybourne M N 1986 *Solid State Commun.* **57** 411–4
Taylor R P, Main P C, Eaves L, Beaumont S P, Thoms S and Wilkinson C D W 1989 *Superlatt. Microstruct.* **5** 575–8
Wharam D A, Thornton T J, Newbury R, Pepper M, Ahmed H, Frost J E F, Hasko D G, Peacock D C, Ritchie D A and Jones G A C 1988 *J. Phys. C: Solid State Phys.* **21** L209–13